Research Article

Yang Gao, Jie Lv, Licheng Liu, and Yingfeng Yu*

# Effect of diacylhydrazine as chain extender on microphase separation and performance of energetic polyurethane elastomer

https://doi.org/10.1515/epoly-2020-0052
received June 10, 2020; accepted July 15, 2020

**Abstract:** It is low cost and feasible to improve the mechanical properties of polyurethane by using the chain extender with hydrogen bonding function to improve the degree of microphase separation. In this article, hydrazine hydrate was used to react with ethylene carbonate and propylene carbonate, respectively, to synthesize diacylhydrazines as the polyurethane chain extender with amide bonds, which were characterized by $^{1}$H nuclear magnetic resonance. Polyurethane with different contents of hard segment were prepared from poly-3,3-bis(azidomethyl)oxetane-tetrahydrofuran as the polyol and 4,4′-diphenylmethane diisocyanate as the isocyanate components. Fourier transform infrared spectroscopy showed that with the increase of the hard segment content, the proportion of hydrogen-bonded ordered carbonyl group increased to 94%, proving that diacylhydrazines could improve the degree of ordered hydrogen bonding, which led to clear microphase separation observed by field emission scanning electron microscopy and higher storage modulus of the polyurethane. Differential scanning calorimetry and dynamic mechanical analysis showed that polyurethane with higher hard segment content is likely to exhibit multiple thermal transitions caused by microphase separation. When the hard segment content was 40%, compared with polyurethane with 1,4-butanediol as the chain extender, the tensile strengths of polyurethanes with diacylhydrazines also improved by 30% and 76%, respectively.

**Keywords:** polyurethane, chain extender, hydrogen bond, microphase separation, thermal-mechanical property

*** Corresponding author: Yingfeng Yu,** State Key Laboratory of Molecular Engineering of Polymers, Department of Macromolecular Science, Fudan University, Shanghai, 200433, China, e-mail: yfyu@fudan.edu.cn
**Yang Gao, Jie Lv, Licheng Liu:** State Key Laboratory of Molecular Engineering of Polymers, Department of Macromolecular Science, Fudan University, Shanghai, 200433, China

## 1 Introduction

Polyurethane elastomer is composed of hard segment with high glass transition temperature ($T_g$) and soft segment with low $T_g$ (1). In the study of the multiblock polyurethane, Cooper and Tobolsky proposed that polyurethane has the bulk structure of microphase separation (2). Due to the thermodynamic incompatibility between the soft segment and the hard segment, microphase separation occurs in polyurethane. Paiksung et al. suggested that the microphase separation in polyurethane is incomplete (3), while the degree of microphase separation has an important impact on mechanical performance of polyurethane elastomer. Mixing of hard and soft segments into the homogenous structure will reduce the application range of materials in low temperature and lead to the decline of heat resistance of polyurethane.

Due to the high directivity and bonding strength, hydrogen bond is conducive to microphase separation and the formation of independent micro regions in soft segments and hard segments. In Hu and coworker's work, a novel supramolecular network with the excellent shape-memory effect was synthesized through the reaction of *N*,*N*-bis(2-hydroxylethyl)isonicotinamine and hexamethylene diisocyanate (4–6). Differential scanning calorimetry (DSC) showed that the microphase separation structure was formed through intermolecular hydrogen bonding. If the content of hydrogen bond can be increased, the microphase separation can be further promoted, and the mechanical performance of the system can be improved (7–9).

Energetic polyurethane and composite materials have been used as solid propellant binders in the past

Open Access. © 2020 Yang Gao *et al.*, published by De Gruyter. This work is licensed under the Creative Commons Attribution 4.0 International License.

few decades (10–12). Composite solid rocket propellant is composed of metal fuel, solid oxidant, binder and other additives (13,14). The polyurethane binder can fix these solid components into ideal shape and complete structure. Its properties have an important impact on the final process properties, energy level and mechanical performance of the propellant (14–16). The introduction of the azide group into energetic polyurethane can increase the heat release and reduce the oxygen consumption and the molecular weight of decomposition products, so it has a high application potential (17). Typical compounds that introduce azides include glycidyl azide polymer (GAP) (18), 3,3-bis-azido methyl oxetane (BAMO) (16,19) and 3-azidomethyl-3-methyl oxetane (AMMO) (20).

GAP-based material can be utilized as a propellant binder (21,22), but its mechanical performance is not ideal. In the study by Zhang et al., the tensile strength of energetic polyurethane with GAP is less than 5 MPa, and the elongation at break is only 50% (18). Optimization of GAP-based polyurethane as a propellant binder is realized by modifying GAP with polycaprolactone (23), tetrahydrofuran (24), nitrocellulose filler (25) and propargyl-terminated polyether (26).

Compared with GAP, azide groups are added to the side chain of BAMO, which improves the energy and the symmetry of the system. However, BAMO homopolymer (PBAMO) is a rigid solid at room temperature, which makes it difficult to mix with other components. So it is necessary to modify PBAMO (15,27). In addition to the introduction of AMMO to modify PBAMO (28), many studies have also introduced tetrahydrofuran (THF) and other groups to modify PBAMO through copolymerization (29–32). The influence of two large volume symmetrical azide groups on the lack of secondary crosslinking is eliminated, and the mechanical performance is improved. Currently, the energetic polyurethane synthesized from BAMO/THF copolymer (poly-3,3-bis(azidomethyl)oxetane-tetrahydrofuran [PBAMO-THF]) has good mechanical performance at low temperature, but it is not ideal at high temperature.

The understanding of the relationship among hydrogen bond, microphase separation and the thermomechanical performance is the key to expand the application of energetic polyurethane as a propellant binder. It is a low-cost, easy-processing and feasible way to introduce the group, which can form hydrogen bond into the chain extender. However, there are few studies on chain extenders that contribute to the formation of hydrogen bonds. In our previous work, we have employed investigations for energetic poly (urethane-urea) copolymers (33). With the increase of hard segment, the proportion of hydrogen-bonded ordered part, the degree of microphase separation and the tensile strength all increased. In this article, diacylhydrazine was synthesized and characterized by $^{1}$H Nuclear magnetic resonance ($^{1}$H NMR). Then, it was introduced into energetic polyurethane elastomer as a chain extender. A series of energetic polyurthane were prepared with PBAMO-THF as the polyol and 4,4′-diphenylmethane diisocyanate (MDI) as the isocyanate. Diacylhydrazine contains amide bonds with latent hydrogen bonding function. Compared with traditional chain extender 1,4-butanediol (BDO), the effects of diacylhydrazine and hard segment content on degree of hydrogen bond ordering, microphase separation, morphology and thermomechanical properties were explored by Fourier transform infrared spectroscopy (FTIR), Field emission scanning electron microscopy (FESEM), DSC and dynamic mechanical analysis (DMA). Furthermore, the effects on the mechanical performance of energetic polyurethane elastomers were studied as well.

# 2 Experimental

## 2.1 Materials

4,4′-Diphenylmethane diisocyanate (MDI, Bayer chemistry) was used as received. PBAMO-THF (Liming Research Institute of Chemical Industry) is the copolymer of 3,3-bis(azidomethyl)oxetane (BAMO) and THF with a Mn of 5,143 g/mol and hydroxyl value at 19.29 mg KOH/g; the monomer ratio of BAMO to THF is 1:1 and polydispersity is 2.80. BDO, *N*,*N*-dimethylformamide (DMF), acetone, ethylene carbonate, propylene carbonate and hydrazine hydrate were purchased from Sinopharm Chemical Reagent Co., Ltd and used without further purification.

## 2.2 Preparation of diacylhydrazines

Hydrazine hydrate was dissolved in acetone and fed into a three-necked flask with a condenser, a magnetic stirrer and a thermostatic bath. The temperature was increased to 80°C under magnetic stirring and kept stable. Then, ethylene carbonate or propylene carbonate was added in

**Table 1:** Composition and $T_g$ of polyurethane elastomers

| Sample name | Chain extender | PBAMO-THF (wt%) | MDI (wt%) | Chain extender (wt%) | $T_{g1}$[a] (°C) | $T_{g1}$[b] (°C) | $T_{g2}$[c] (°C) |
|---|---|---|---|---|---|---|---|
| BDO-20% | BDO | 80 | 16 | 4 | −48 | −34 | – |
| BDO-30% | BDO | 70 | 23 | 7 | −48 | −37 | – |
| BDO-40% | BDO | 60 | 30 | 10 | −48 | −39 | – |
| HCAHE-20% | HCAHE | 80 | 13 | 7 | −49 | −36 | – |
| HCAHE-30% | HCAHE | 70 | 19 | 11 | −48 | −35 | 136 |
| HCAHE-40% | HCAHE | 60 | 25 | 15 | −47 | −35 | 145 |
| HCAHP-20% | HCAHP | 80 | 13 | 7 | −48 | −37 | – |
| HCAHP-30% | HCAHP | 70 | 18 | 12 | −47 | −36 | 140 |
| HCAHP-40% | HCAHP | 60 | 23 | 17 | −47 | −36 | 141 |

[a] $T_g$ of the soft segment by DSC. [b] $T_g$ of the soft segment by DMA. [c] $T_g$ of the hard segment by DMA.

a molar ratio of 2:1 to hydrazine hydrate. After reaction for 24 h, acetone and other solvents were removed by rotary evaporation. The product of hydrazine hydrate and ethylene carbonate was 1,2-hydrazinedicarboxylic acid, 1,2-bis(2-hydroxyethyl) ester (HCAHE). The product of hydrazine hydrate and propylene carbonate was named HCAHP, which was a mixture of 1,2-hydrazinedicarboxylic acid, bis(2-hydroxypropyl) ester, 1,2-hydrazinedicarboxylic acid, 1-(2-hydroxypropyl) 2-(2-hydroxy-1-methylethyl) ester and 1,2-hydrazinedicarboxylic acid, 1,2-bis(2-hydroxy-1-methylethyl) ester. HCAHE is solid, whereas HCAHP is liquid at room temperature (K Eberhard, June 2001, Stabilized blocked isocyanates and their use in polyurethane stoving lacquers, U.S. patent 6,242,530).

## 2.3 Preparation of polyurethane elastomer

PBAMO-THF was heated at 120°C, dehydrated by vacuum agitation for 30 min and cooled to room temperature. Then, MDI was added under the protection of nitrogen. The system was stirred and heated to 70°C. After reaction for 4 h, the

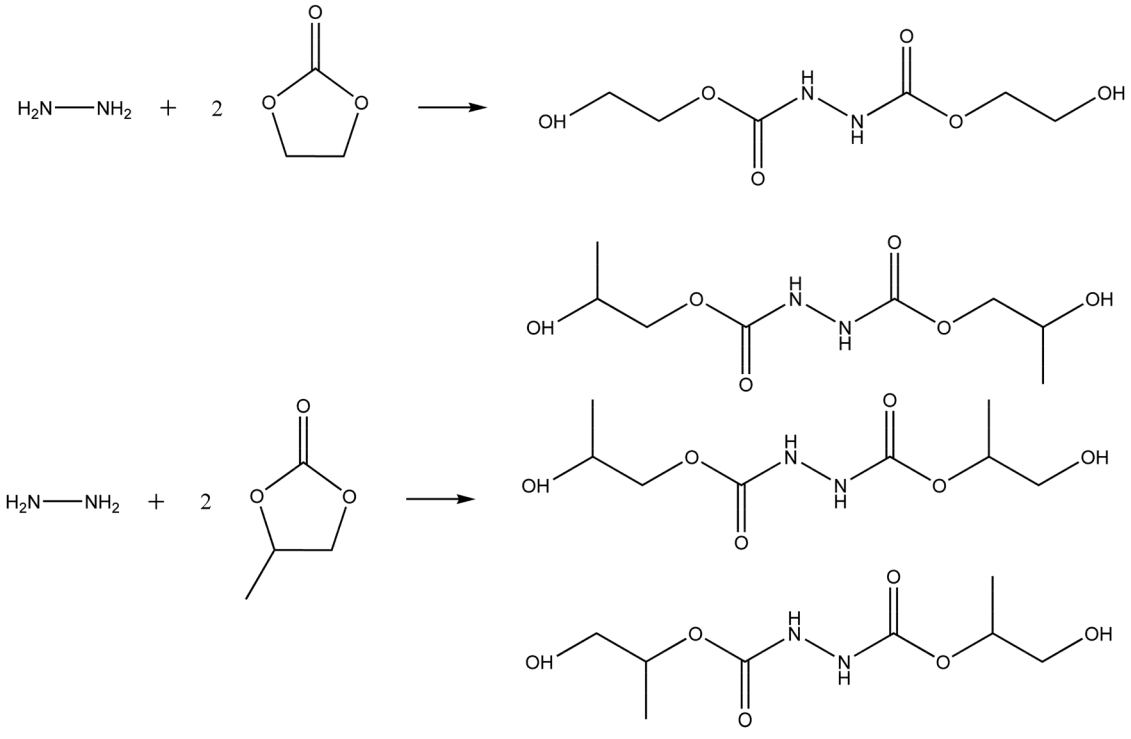

**Scheme 1:** Chemical structure of reactants and products.

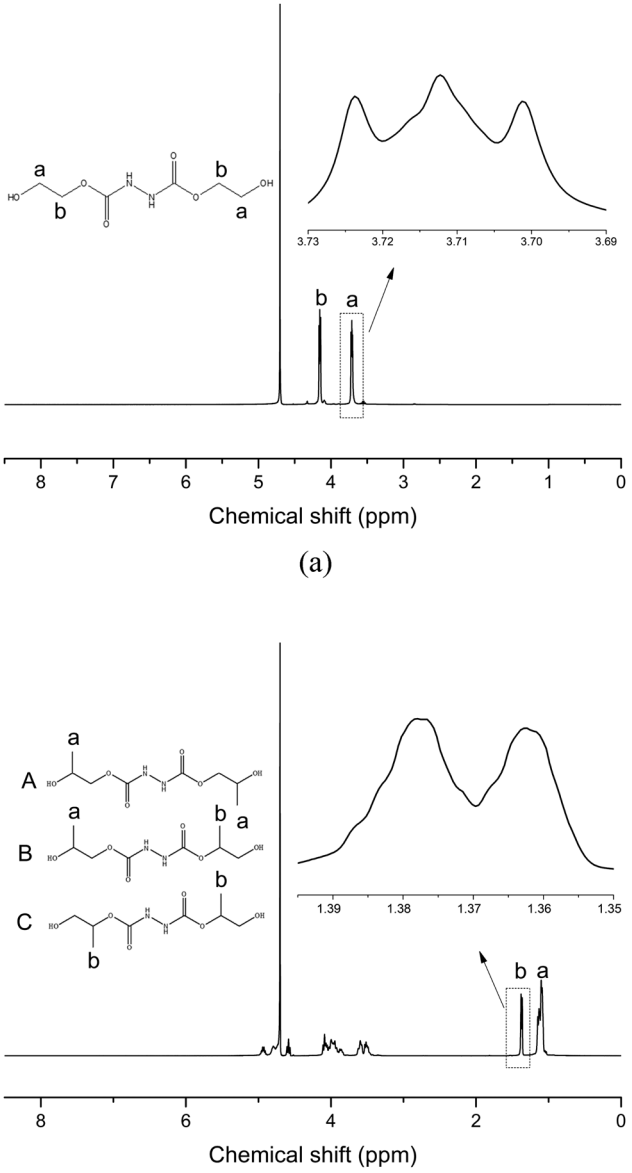


**Figure 1:** Structural formula and $^1$H NMR of (a) HCAHE and (b) HCAHP.

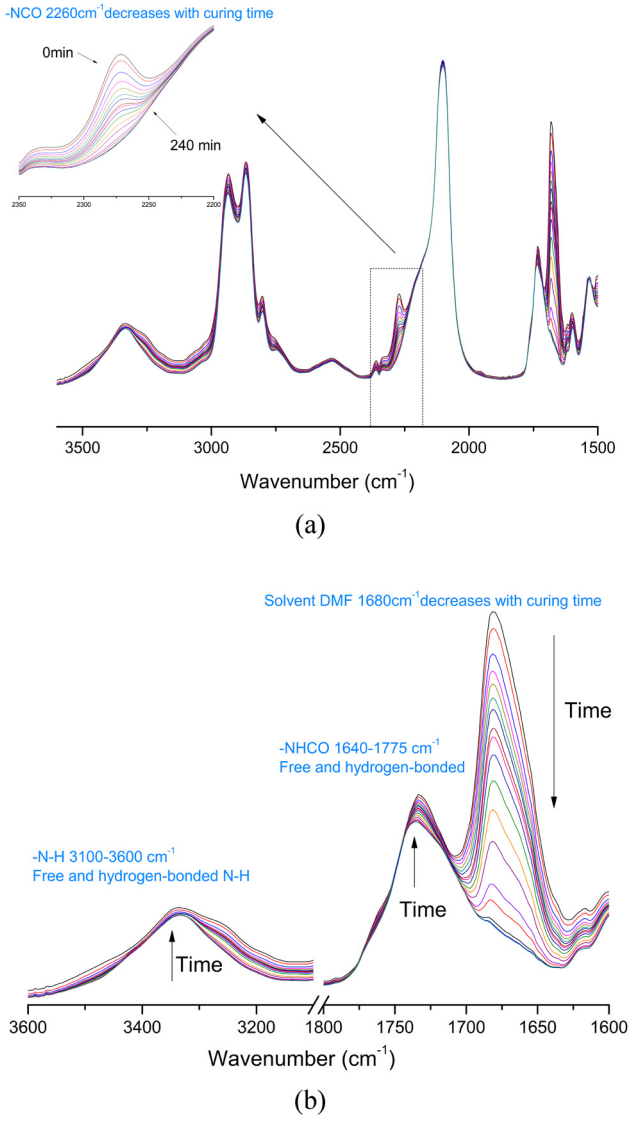


**Figure 2:** *In situ* curing FTIR spectra for HCAHE-20% at 60°C in 4 h: (a) NCO group region and (b) N–H and C=O group region.

product was cooled and sealed to obtain prepolymer. The chain extender HCAHE or HCAHP or BDO was dissolved in DMF, heated to 120°C and stirred for 2 h under the protection of nitrogen. After cooling to room temperature, the prepolymer was added. The mixture was stirred evenly and cured at 60°C for 24 h and then placed in a desiccator at room temperature for 7 days to obtain the polyurethane elastomers. The proportions of PBAMO-THF, MDI and chain extender are presented in Table 1. Polyurethanes with hard segment contents of 20%, 30% and 40% were obtained. The polyurethanes with BDO as a chain extender were named BDO-20%, BDO-30% and BDO-40%. The polyurethanes with HCAHE as a chain extender were named HCAHE-20%, HCAHE-30% and HCAHE-40%, while the polyurethanes with HCAHP as a chain extender were named HCAHP-20%, HCAHP-30% and HCAHP-40%.

## 2.4 Characterization

### 2.4.1 $^1$H NMR

$^1$H NMR spectra were recorded on an AVANCE III HD NMR (Bruker, Switzerland) with deuterated water ($D_2O$) as a solvent. Test conditions are as follows: sample

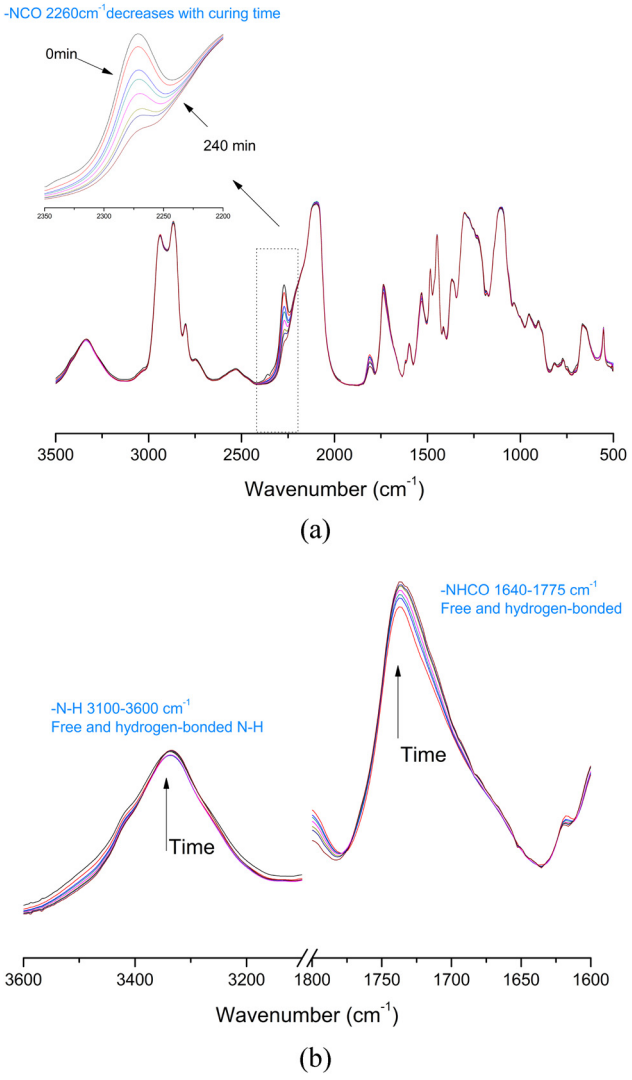


**Figure 3:** *In situ* curing FTIR spectra for HCAHP-20% at 60°C in 4 h: (a) NCO group region and (b) N–H and C=O group region.

quantity, 5–10 mg; the inner diameter of tube used in the test, 5 mm; the volume, 0.5 mL; scanning time, 4; temperature, 25°C.

### 2.4.2 FTIR

FTIR was used to track the curing process of polyurethane with Nicolet 6700 (Thermofisher, USA). The chain extenders were fully mixed with prepolymers and coated on KBr salt tablets. The sample was cured at 60°C in 4 h. The fully cured polyurethane elastomers were characterized by FTIR as well. Test conditions were as follows: mid-infrared 4,000–400 $cm^{-1}$, 64 scanning times, resolution 4 $cm^{-1}$.

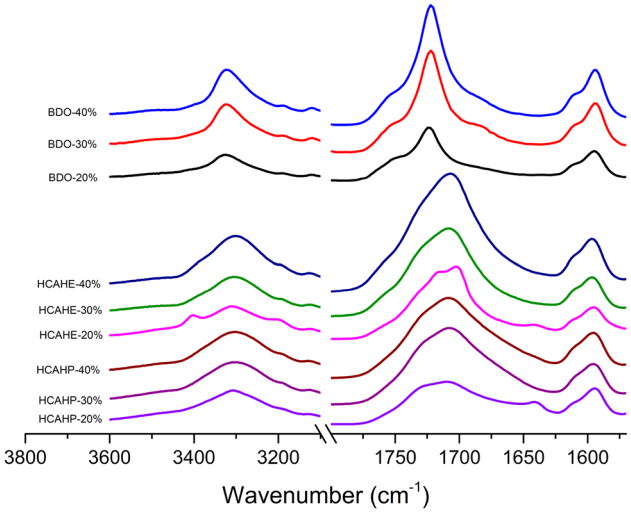


**Figure 4:** FTIR spectra of polyurethane elastomer after curing.

### 2.4.3 FESEM

The fully cured polyurethane was fractured in liquid nitrogen. The fracture surface was coated with a layer of gold of 5–7 nm thick by an ion sputtering instrument. Then, the surface morphology of polyurethane elastomers was observed by Ultra 55FESEM (Zeiss, Germany). The test voltage was set to 5 kV. The magnification is 1,000× and 5,000×.

### 2.4.4 DSC

The thermal transition of polyurethane elastomer was measured by Q2000 (TA, USA) with the nonisothermal DSC method. The sample quantity was 5–10 mg each time, and the measurement was carried out in a solid sealed sample disk in the atmosphere of nitrogen. The heating range was from −80°C to 200°C with a heating rate of 10°C/min.

### 2.4.5 DMA

The storage modulus and loss factor (tan $\delta$) of polyurethane elastomers were measured by SDTA861e (Mettler Toledo, Switzerland). The sample size was 10 × 6 × 5 $mm^3$. Test conditions were as follows: tensile mode, 1 Hz frequency; 1 N dynamic force; and 100 µm displacement. The atmosphere was air. The heating range was from −80°C to 200°C with a heating speed 3°C/min.

### 2.4.6 Tensile test

Tensile strength and elongation at break of polyurethane elastomer were measured by Instron 5966 (American Instron,

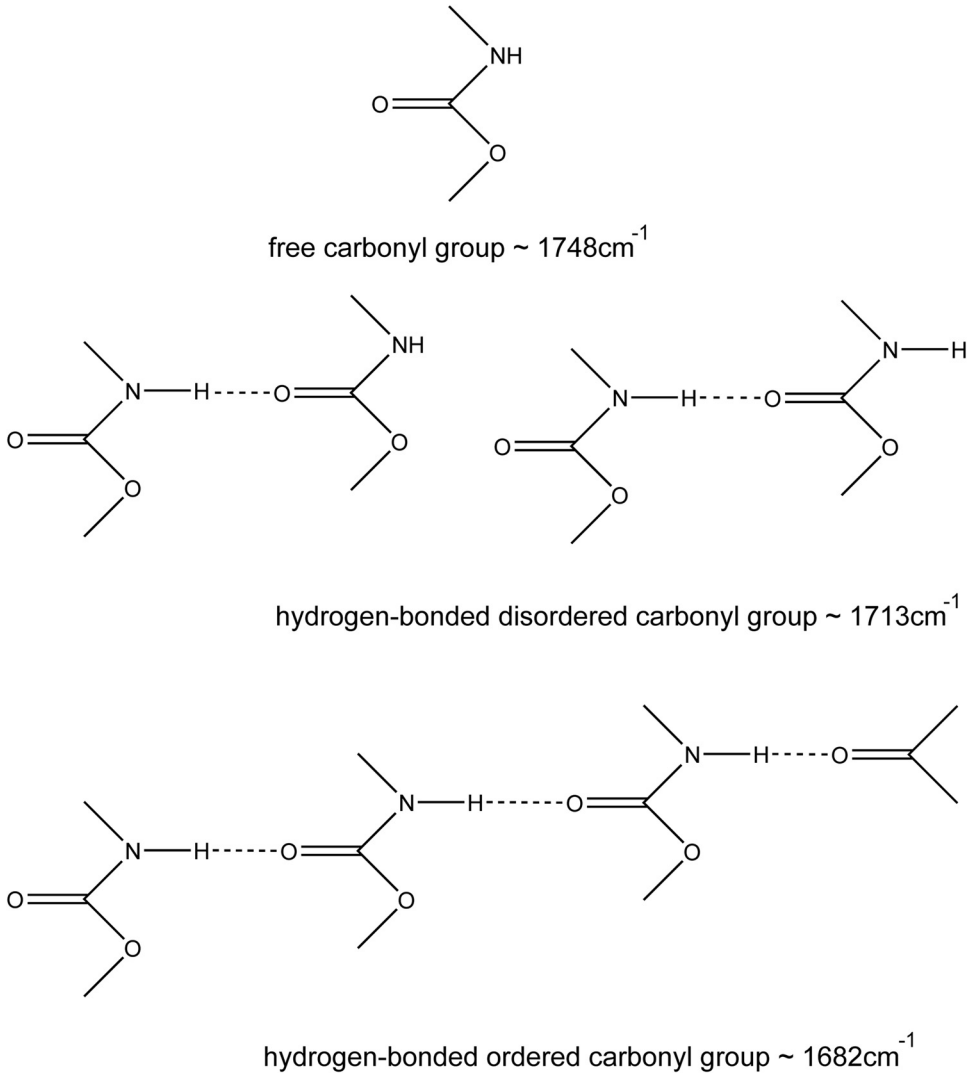


**Figure 5:** Band assignments for the carbonyl group of polyurethane.

USA). The samples were prepared according to ASTM D638-96. The data reported were the mean value of five specimens, and the standard deviation was calculated. Test conditions were as follows: tensile speed, 50 mm/min; temperature, 25°C; relative humidity, about 60% h.

# 3 Results and discussion

## 3.1 Characterization of HCAHE/HCAHP

Hydrazine hydrate reacts with ethylene carbonate and propylene carbonate (as shown in Scheme 1). There is only one structural formula for HCAHE, while there are three possible structural formulas for HCAHP.

To verify the reaction of hydrazine hydrate with ethylene carbonate or propylene carbonate, the synthesized products were characterized by $^1$H NMR, as shown in Figure 1. The peak at a chemical shift of $\delta$ 4.80 is the solvent $D_2O$ peak. In the $^1$H NMR spectrum of HCAHE, the peaks of $\delta$ 3.71 and $\delta$ 4.15 are hydrogen atoms from methylene groups. Affected by adjacent methylene, the proton absorption peak of methylene splits into triplet peak. In the $^1$H NMR spectrum of HCAHP, the peaks of $\delta$ 1.12 and $\delta$ 1.37 are methyl hydrogen. The peak splitting indicates that there is a proton on the adjacent carbon. Due to the three possible structures of HCAHP, the broad peaks of $\delta$ 3.50–4.90 are different hydrogen atoms forming methylene and methyne. The proportion range of the three structures can be calculated according to the ratio of the area of $-CH_3$ proton peak at $\delta$ 1.12 and $\delta$ 1.37 since the methylene proton peak, the methyne proton peak of HCAHP and the solvent $D_2O$ peak overlap due

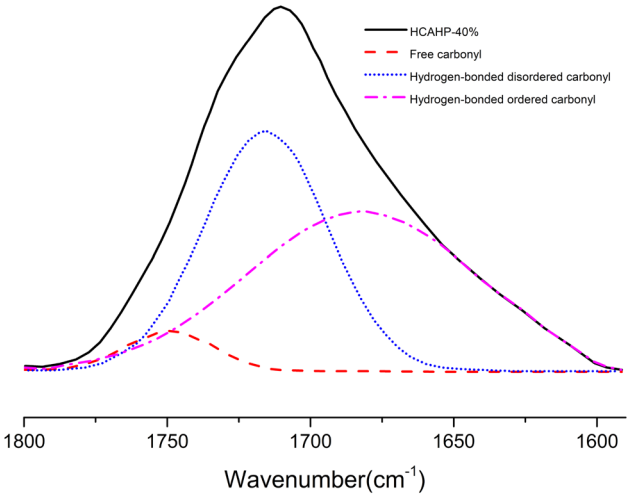


**Figure 6:** Peak fitting by origin in C=O region of the FTIR spectra of HCAHP-40%.

to the similar $\delta$ values and multiplicities, which makes it difficult to calculate the ratio quantitatively. The proportion of structure A is 48.2–74.1%, that of structure B is 0–51.8% and that of structure C is 0–25.9% (structures A/B/C are shown in Figure 1). It can be seen that the $^1$H NMR spectrum of the product is consistent with its molecular structure. The chain extenders HCAHE and HCAHP containing amide bonds were synthesized successfully.

## 3.2 Analysis of microphase separation

The synthesized chain extenders HCAHE and HCAHP were introduced into the energetic polyurethane elastomer with PBAMO-THF as a soft segment and MDI as diisocyanate. Figures 2 and 3 show the *in situ* curing FTIR spectra of HCAHE-20% and HCAHP-20% in different wavenumber ranges at 60°C. The absorption peak near 2,270 cm$^{-1}$ corresponds to the stretching vibration of the unsaturated bond in –NCO and the typical peak of an NCO group. The peak area decreases significantly with the curing process, which represents the consumption of isocyanate groups. HCAHE is solid at room temperature and insoluble in prepolymer, so it needs to be dissolved by DMF to participate in reaction. There will be an obvious C=O stretching vibration absorption peak at 1,680 cm$^{-1}$, which corresponds to DMF and gradually decreases with the curing process. HCAHP is liquid at room temperature, and it can be directly mixed with prepolymer. With the reaction of –NCO and –OH, there are obvious increases in the half peak width of the N–H stretching vibration absorption

**Table 2:** Quantitative analysis in the C=O region of the FTIR spectra

| Samples | Relative absorbance of C=O groups in polyurethane | | |
|---|---|---|---|
| | 1,748 cm$^{-1}$ | 1,713 cm$^{-1}$ | 1,682 cm$^{-1}$ |
| BDO-20% | 37.9% | 54.2% | 7.9% |
| BDO-30% | 20.9% | 73.2% | 5.9% |
| BDO-40% | 21.4% | 76.2% | 2.4% |
| HCAHE-20% | 4.1% | 64.0% | 31.9% |
| HCAHE-30% | 0.3% | 50.3% | 49.4% |
| HCAHE-40% | 0.4% | 5.0% | 94.6% |
| HCAHP-20% | 7.1% | 71.4% | 21.5% |
| HCAHP-30% | 5.6% | 51.0% | 43.4% |
| HCAHP-40% | 5.2% | 42.2% | 52.6% |

peak (3,100–3,600 cm$^{-1}$). Taking 3,300 cm$^{-1}$ as the peak center, the N–H bonds at the later stage of curing reaction contains more N–H bonds with low wave number. Since the N–H bonds form more ordered hydrogen bonds and make the N–H absorption peak move to low wave number. The peak intensity from 1,640 to 1,775 cm$^{-1}$, which corresponds to C=O stretching vibration and N–H bending vibration also increases with the curing time, which reveals the formation of carbamate. The change of the C=O region to low wavenumber region reflects the process of hydrogen bond ordering.

To study the relationship among the chain extender, hard segment content and the degree of hydrogen bond ordering, the fully cured polyurethane was characterized by FTIR, as shown in Figure 4. The proportion of the carbonyl forming hydrogen bond and the degree of hydrogen bond ordering can be quantitatively calculated by studying the absorption peak of carbonyl in

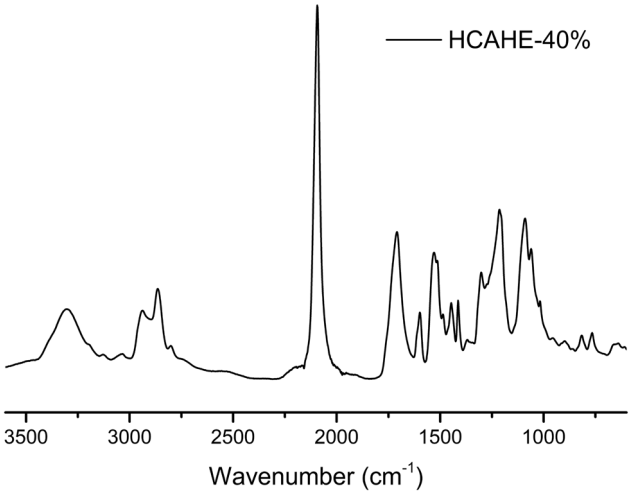


**Figure 7:** FTIR spectra of fully cured HCAHE-40%.

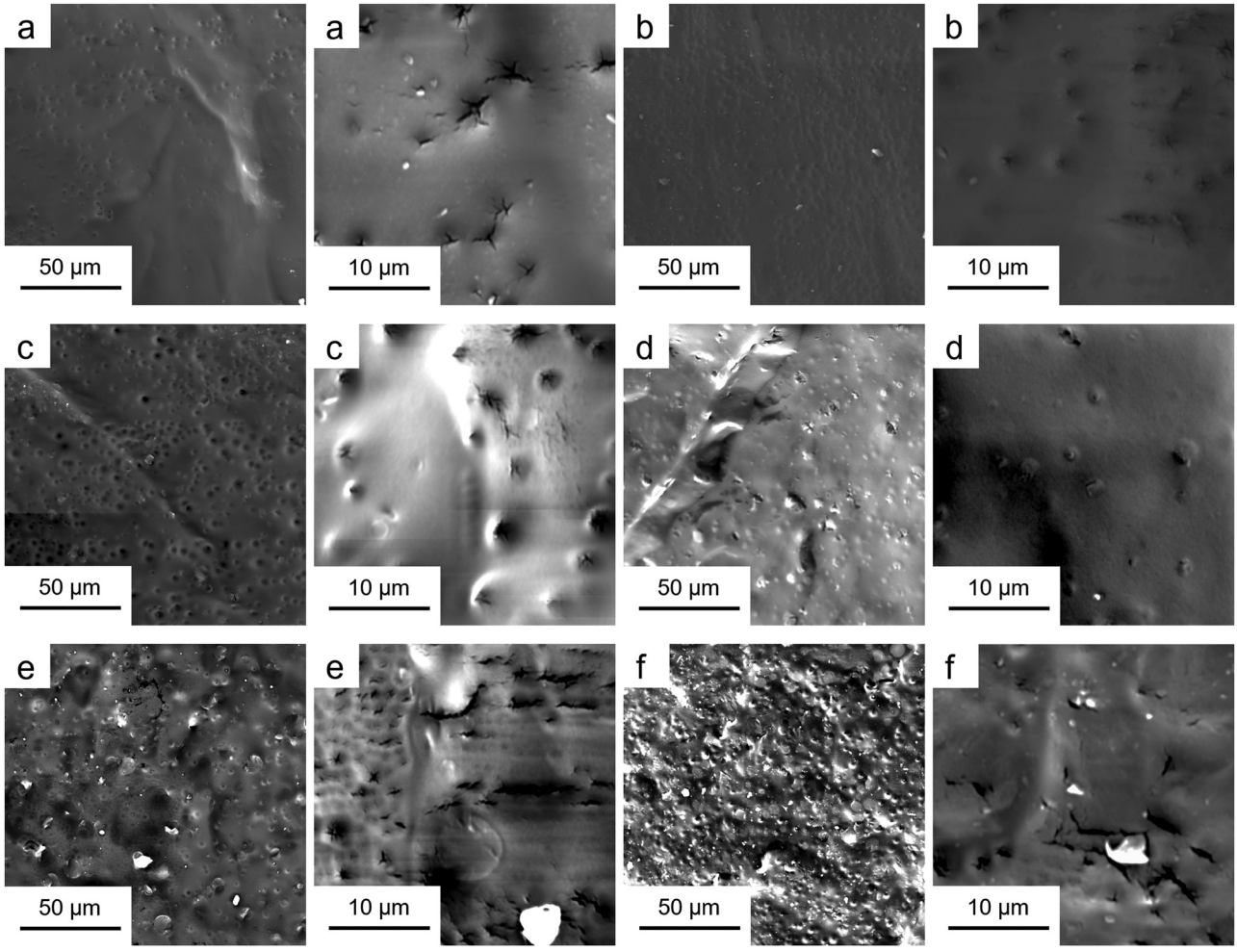


**Figure 8:** FESEM images of polyurethane elastomers: (a) HCAHP-20%, (b) HCAHP-30%, (c) HCAHP-40%, (d) HCAHE-20%, (e) HCAHE-30% and (f) HCAHE-40%.

polyurethane. In the study by Yilgor et al., peak fitting was used to determine the peak area of a specific C=O. Then, the area was divided by the total area to get the percentage. Among the C=O stretching vibration absorption peaks, 1,733, 1,708 and 1,696 $cm^{-1}$ are considered to be free carbonyl, hydrogen-bonded disordered carbonyl and ordered carbonyl (34). The corresponding peak position of our work was defined, as shown in Figure 5. Peak fitting by origin was used to get the area of the corresponding peak, as shown in Figure 6. Substitute the peak area into Eq. 1 to obtain the percentage of free, hydrogen-bond disordered and ordered C=O groups in polyurethane.

$$\text{C=O}(1{,}748)\% = \frac{A(1{,}748)}{A(1{,}748) + A(1{,}713) + A(1{,}682)} \quad (1)$$

By the quantitative analysis, the percentage of different C=O in polyurethane samples is presented in Table 2. Compared with BDO-cured polyurethanes, the diacylhydrazine-cured polyurethanes obviously contain more carbonyls with lower wave number. For samples containing the same diacylhydrazine, the percentage of hydrogen-bonded carbonyl increased with the hard segment content, while the free carbonyl decreased. The content of the ordered hydrogen bond formed by carbonyl also increased. For instance, in the hydrogen-bonded ordered carbonyl absorption peak of 1,682 $cm^{-1}$, the relative area was 31.97% for HCAHE-20%, 49.46% for HCAHE-30% and 94.64% for HCAHE-40%. With the increase of the hard segment content, more HCAHP and HCAHE were introduced into the main chain of polyurethane elastomer. The amide hydrogen in the chain extender can form hydrogen bond with carbamate carbonyl or ether in soft segment, thus increasing the content of the hydrogen bond and the degree of ordered hydrogen bonding. Since HCAHE is more symmetrical

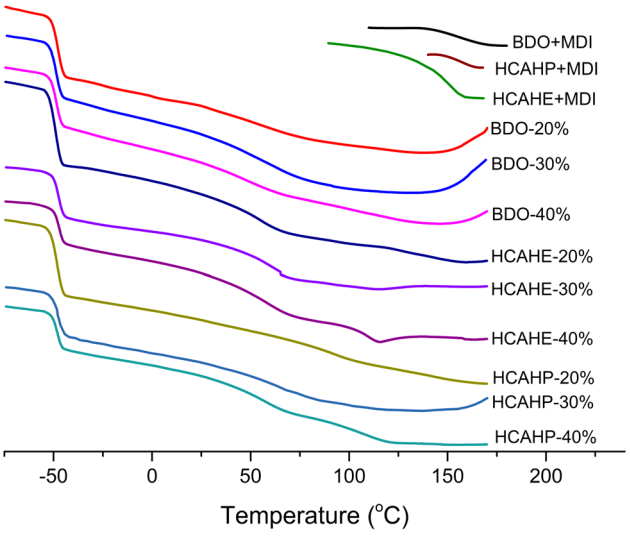


**Figure 9:** Thermal transition of polyurethane elastomer with different hard segment contents and different chain extenders by DSC.

than HCAHP in the molecular structure, the polyurethane with HCAHE formed more ordered hydrogen bonds than the polyurethane with HCAHP.

Figure 7 shows the FTIR spectra of the fully cured HCAHE-40%. The peak at 2,100 $cm^{-1}$ corresponded to the stretching vibration absorption peak of unsaturated bond of nitrogen and nitrogen in azido groups. The $-N_3$ peak with highest intensity shown in Figure 7 proved that the series of polyurethane in our study was energetic polyurethane, which could meet the requirements of high-energy propellant. Due to the easy and environmentally friendly processing, high energy based on energetic $-N_3$ groups and contribution to the low signature, polyurethanes studied in this study have potential application as binders in solid rocket propellants.

Observation of the surface morphology of the fully cured polyurethane is helpful to judge the microphase separation directly. Morphology is also closely related to the final properties of the product (35). In the study by Saha et al., the morphological analysis of drug–nanoclay for controlled drug delivery was well studied (36). Figure 8 shows the FESEM images of polyurethane containing HCAHE/HCAHP. It can be clearly observed that with the increase of the hard segment content, the number of dispersed phase particles from microphase separation increased rapidly. The hard segments tend to be separated from the soft matrix instead of mixing with soft segments. The change of morphology and structure will obviously affect the mechanical properties and dynamic mechanical performance of polyurethane elastomer. With the increase of hard segment particles in the dispersed phase, it can be predicted that the tensile strength of the material will increase significantly, while elongation at break and other properties will depend on the degree of microphase separation.

## 3.3 Thermal-mechanical properties

The thermal transition of the polyurethane samples was investigated by DSC, as shown in Figure 9. For all polyurethanes, the glass transition of the soft segment can be clearly observed, and the corresponding $T_g$ was presented in Table 1. Pure hard segment was the product of the corresponding chain extender and MDI. In the polyurethane elastomer containing hydrogen bonding chain extender, the thermal transition of dissociation can be observed in the short-range and long-range ordered hard segments. For example, in the DSC curve of HCAHE-40%, three kinds of thermal transitions can be observed: glass transition of soft segment near −50°C, dissociation of short-range ordered hard segment near 60°C and dissociation of long-range ordered hard segment near 110°C. In the DSC curve of BDO-40%, there are two thermal transitions, which are the glass transition of the soft segment near −50°C and the dissociation of the corresponding short-range ordered hard segment near 60°C, but there is no obvious thermal transition of the long-range ordered hard segment dissociation. It is observed by comparison that when the content of the hard segment is 40%, HCAHE samples have more long-range ordered hard segment structure than BDO samples. For polyurethane elastomers with the same kind of chain extender containing hydrogen bond, with the increase of the hard segment content (i.e., the increase of the amount of the chain extender), it is easier to observe the thermal transformation near 110°C, corresponding to the dissociation of long-range ordered hard segments. Due to the amide bond in HCAHE/HCAHP, the introduction of hydrogen bond into polyurethane elastomer is conducive to the formation of ordered hydrogen bond.

The storage modulus of polyurethane elastomer was monitored by DMA, as shown in Figure 10. The storage modulus at −50°C and 25°C was presented in Table 3. The glass transitions of the soft and hard segment were observed in HCAHP-30% and HCAHP-40% at around −36°C and 140°C. However, thermal transition of hard segment was unavailable in HCAHP-20%, which

reflected inadequate microphase separation. The storage modulus after glass transition of soft segment reflects the physical crosslinking strength of polyurethane. Storage modulus of HCAHE/HCAHP-cured polyurethane at 25°C was generally larger than that of BDO-cured polyurethane. The modulus after $T_g$ of soft segment increased with the hard segment content. Since the connectivity of the hard segment domain increased, a continuous hard micro domain structure formed, which contained both hydrogen-bonded disordered part and ordered part. With the increase of the hard segment content, the hydrogen bonds formed physical crosslinks with higher intensity to reinforce the structure of polyurethane.

The loss factor (tan $\delta$) was further measured by DMA, and the corresponding $T_g$ of each sample is presented in Table 1. In HCAHP-30%, HCAHE-30%, HCAHP-40% and HCAHE-40%, the glass transition of hard segment could be easily observed, while the situation was opposite in HCAHP-20%-, HCAHE-20%- and BDO-cured polyurethanes.

As presented in Table 1, there is no significant difference in the $T_g$ of the soft segment of all the polyurethane elastomers, which are around −36°C. The thermal transitions of polyurethane elastomers were compared by tan $\delta$ curves, as shown in Figure 11. For HCAHE-40% and HCAHP-40%, there is a steep peak that represents glass transition in the hard segment near 140°C. For BDO-cured polyurethane, there is only a very gentle peak in the range of 100–150°C, which means the glass transition of the hard segment is not clear. For polyurethane containing HCAHE/HCAHP, with the increase of the hard segment content, the maximum tanδ is getting higher at $T_g$ of the hard segment. Therefore, the introduction of HCAHP and HCAHE is conducive to microphase separation and the formation of independent soft and hard segments, which leads to clear glass transition of hard segments.

$T_g$ shift was closely related to the degree of microphase seperation. The closer the $T_g$ value of the hard segment is to that of the pure hard polymer, the fewer the hard segment is dissolved in the soft segment. Taking HCAHE-cured polyurethane as an example, the $T_g$ values of the hard segment of HCAHE-30% and HCAHE-40% are 136°C and 145°C, respectively, while the $T_g$ of the pure hard polymer (HCAHE + MDI) is 146°C. With the increase of the hard segment content, hard segment tends to self-associate to form hard domain rather than mixing in the soft segment, which contributes to microphase separation and closer $T_g$ of hard segment.

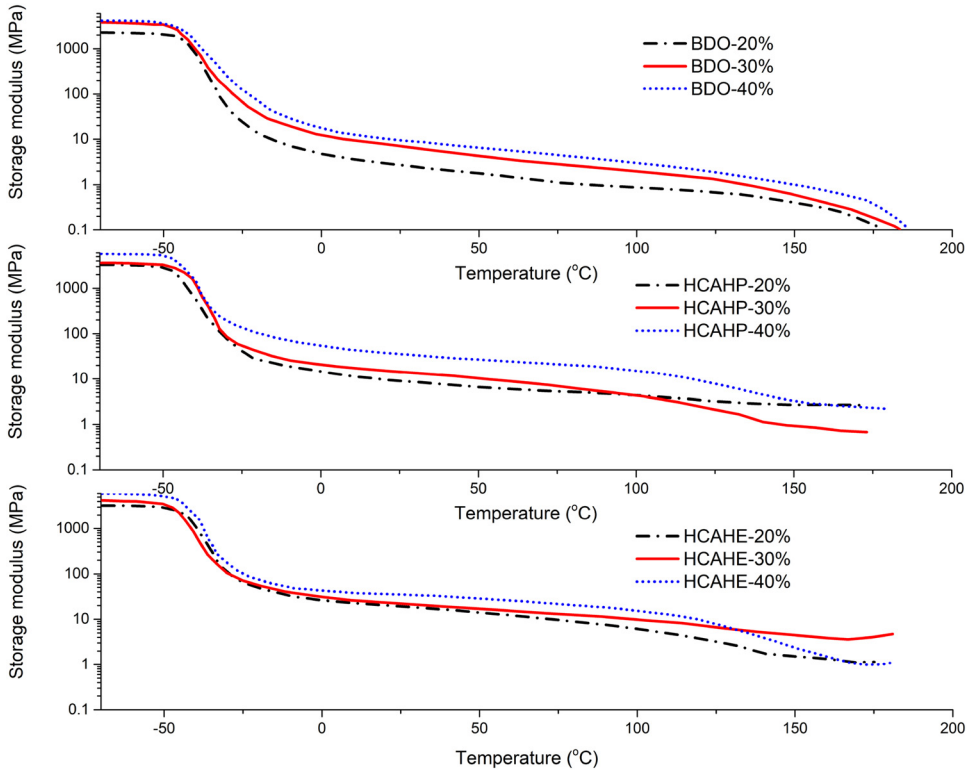


**Figure 10:** Storage modulus curves of polyurethane elastomers by DMA.

**Table 3:** Mechanical performance of polyurethane elastomers

| Sample name | Storage modulus at −50°C (GPa) | Storage modulus at 25°C (MPa) | Elongation at break (%) | Tensile strength (MPa) |
|---|---|---|---|---|
| BDO-20% | 3.6 | 2.4 | 580 ± 70[a] | 5.1 ± 0.2 |
| BDO-30% | 3.4 | 7.0 | 700 ± 60 | 7.4 ± 0.4 |
| BDO-40% | 2.1 | 9.5 | 450 ± 40 | 11.0 ± 0.2 |
| HCAHE-20% | 2.9 | 20.3 | 400 ± 30 | 4.7 ± 0.3 |
| HCAHE-30% | 3.5 | 22.1 | 640 ± 50 | 11.4 ± 0.5 |
| HCAHE-40% | 5.2 | 35.0 | 450 ± 30 | 19.4 ± 2.2 |
| HCAHP-20% | 2.9 | 8.5 | 410 ± 10 | 3.4 ± 0.2 |
| HCAHP-30% | 3.3 | 14.0 | 610 ± 30 | 9.5 ± 0.4 |
| HCAHP-40% | 5.3 | 33.1 | 370 ± 10 | 14.3 ± 0.1 |

[a] Standard deviation.

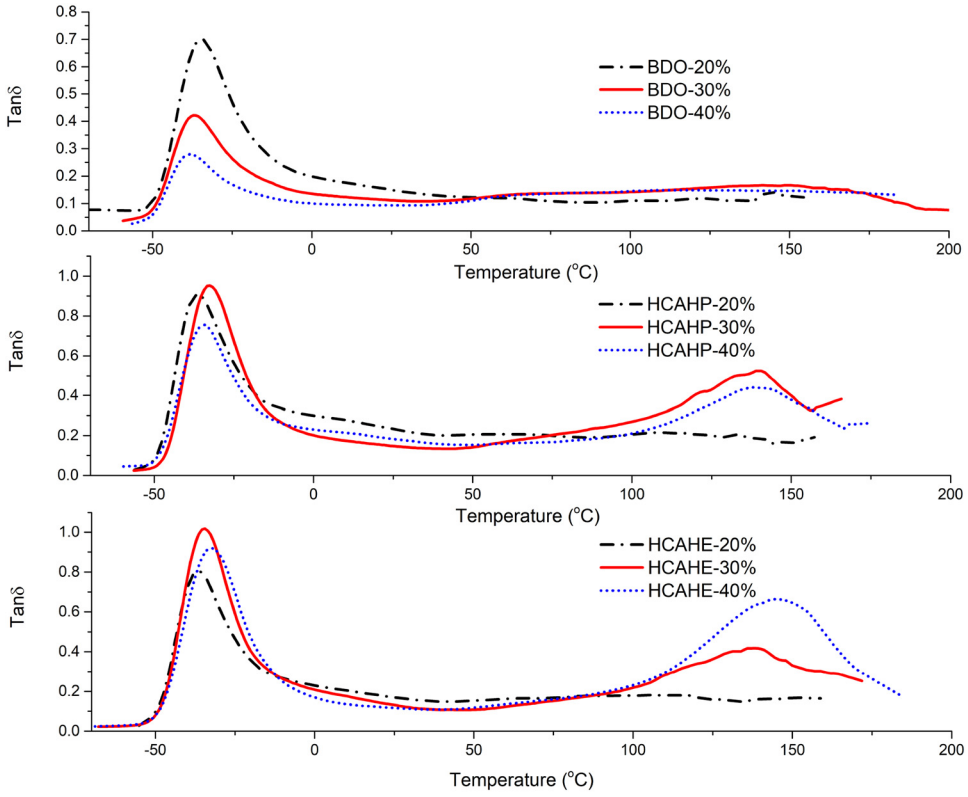


**Figure 11:** tan $\delta$ curves of polyurethane elastomers by DMA.

Finally, the mechanical performance of polyurethane was monitored by tensile test, as listed in Table 3. Among the three chain extender systems, the elongation at break of polyurethane elastomer with the same chain extender reaches the maximum value at 30% hard segment content. When the hard segment content is 40%, the elasticity is greatly reduced. The elasticity of polyurethane is mainly provided by the soft segment, which is rarely affected by the percentage of the hard segment. In contrast, the tensile strength of the polyurethane elastomer increased with the hard segment content. For instance, the tensile strengths of HCAHE-20%, -30%, -40% were 4.7, 11.4 and 19.4 MPa, respectively. For polyurethane elastomer with 30% and 40% hard segment content, the tensile strength of the polyurethane elastomer with HCAHE and HCAHP is higher than that of polyurethane with the BDO chain extender, since more HCAHE/HCAHP with amide bond is introduced into the molecular structure of polyurethane. The intermolecular interaction was enhanced, and more

ordered hydrogen bonds were formed, which led to more physical crosslinks and higher tensile strength.

The mechanical performance is consistent with the previous test results. The introduction of N–H bond into the main chain of polyurethane is conducive for improving the degree of hydrogen bonding in the material, further promoting the microphase separation to form a hard segment crystal area and improving its mechanical performance. Because of the better symmetry of HCAHE than HCAHP, the tensile strength of HCAHE-cured elastomers is larger than that of HCAHP-cured elastomers.

For the application of polyurethane in binders, the mechanical property of the binder plays a decisive role compared to that of the propellants since all the components in the composite propellant are dispersed in the binder. The propellant should have good mechanical properties at low temperature and good thermal stability at high temperature (10,16,21). Compared with BDO-cured polyurethane, HCAHE/HCAHP-cured polyurethane has higher storage modulus at both low and high temperatures. The polyurethane cured with HCAHE/HCAHP can maintain its stability at 170°C without decomposition, and the tensile strength also improved. All these factors make HCAHE/HCAHP have a certain application potential in the field of propellant binders.

## 4 Conclusion

The studies on microphase separation and a new chain extender for energetic polyurethane are of great significance to scientific research and engineering application. In this article, chain extenders HCAHE/HCAHP with the diacylhydrazine group were synthesized, characterized and introduced into energetic polyurethane elastomer. FTIR showed that with the increase of the hard segment content, the proportion of the hydrogen-bonded ordered carbonyl group increased, proving that HCAHE/HCAHP could improve the degree of ordered hydrogen bonding. Thermal transition $T_g$ and storage modulus were further studied by DSC and DMA. With the increase of the HCAHE/HCAHP content, hard segment tended to self-associate to form independent hard domain from the soft segment, which contributed to microphase separation and clear glass transition of the hard segment in polyurethane. Compared with the traditional chain extender BDO, the tensile strength of polyurethane with HCAHE was also significantly improved.

Both HCAHE and HCAHP are diacylhydrazine with amide hydrogen, which can form hydrogen bond with carbamate carbonyl, increase the percentage of ordered hydrogen bond and lead to microphase separation and physical crosslinks, thus improving the mechanical performance of energetic polyurethane. HCAHE/HCAHP-cured polyurethane was proved to be energetic polyurethane with improved mechanical properties at high and low temperatures. By optimization of the structure of diacylhydrazine with amide bonds, HCAHE and HCAHP are expected to be potential chain extenders for polyurethane as propellant binders.

**Acknowledgments:** The authors received no financial support for the research, authorship and/or publication of this article.

## References

(1) Bonart R, Muller EH. Phase separation in urethane elastomers as judged by low-angle X-Ray-scattering. 2. Experimental results. J Macromol Sci B. 1974;10(2):345–57. doi: 10.1080/00222347408260835.

(2) Cooper SL, Tobolsky AV. Properties of linear elastomeric polyurethanes. J Appl Polym Sci. 1966;10(12):1837–44. doi: 10.1002/app.1966.070101204.

(3) Paiksung CS, Hu CB, Wu CS. Properties of segmented poly (urethaneureas) based on 2,4-toluene diisocyanate. 1. thermal transitions, X-ray studies, and comparison with segmented poly(urethanes). Macromolecules. 1980;13(1):111–6. doi: 10.1021/ma60073a022.

(4) Chen SJ, Hu JL, Zhuo HT, Yuen CWM, Chan LK. Study on the thermal-induced shape memory effect of pyridine containing supramolecular polyurethane. Polymer. 2010;51(1):240–8. doi: 10.1016/j.polymer.2009.11.034.

(5) Chen SJ, Hu JL, Yuen CWM, Chan LK. Fourier transform infrared study of supramolecular polyurethane networks containing pyridine moieties for shape memory materials. Polym Int. 2010;59(4):529–38. doi: 10.1002/pi.2732.

(6) Chen SJ, Hu JL, Yuen CWM, Chan LK. Supramolecular polyurethane networks containing pyridine moieties for shape memory materials. Mater Lett. 2009;63(17):1462–4. doi: 10.1016/j.matlet.2009.03.028.

(7) Liu ST, Tian M, Yan BY, Yao Y, Zhang LQ, Nishi T, et al. High performance dielectric elastomers by partially reduced graphene oxide and disruption of hydrogen bonding of polyurethanes. Polymer. 2015;56:375–84. doi: 10.1016/j.polymer.2014.11.012.

(8) Houton KA, Burslem GM, Wilson AJ. Development of solvent-free synthesis of hydrogen-bonded supramolecular polyurethanes. Chem Sci. 2015;6:2382–8. doi: 10.1039/C4SC03804E.

(9) Jiang B, Tsavalas JG, Sundberg DC. Morphology control in surfactant free polyurethane/acrylic hybrid latices – The

special role of hydrogen bonding. Polymer. 2018;139:107–22. doi: 10.1016/j.polymer.2018.01.054.
(10) Sekkar V, Raunija TSK. Hydroxyl-terminated polybutadiene-based polyurethane networks as solid propellant binder-state of the art. J Propul Power. 2015;31(1):16–35. doi: 10.2514/1.B35384.
(11) Govindan G, Athithan SK. Studies on curing of polyurethane propellant binder system. Propell Explos Pyrot. 1994;19(5):240–4. doi: 10.1002/prep.19940190505.
(12) Ahmed AI, Ali AA, El-Masry AM, Tawfik SM. Development of polyurethane-based solid propellants using nanocomposite materials. Propell Explos Pyrot. 2016;41(2):286–94. doi: 10.1002/prep.201500182.
(13) Hoffman DM, Caley LE. Polymer blends as high explosive binders. Polym Eng Sci. 1986;26(21):1489–99. doi: 10.1002/pen.760262105.
(14) Sikder AK, Reddy S. Review on energetic thermoplastic elastomers (ETPES) for military science. Propell Explos Pyrot. 2013;38(1):14–28. doi: 10.1002/prep.201200002.
(15) Luo Y, Chen P, Zhao FQ, Hu RZ, Li SW, Gao Y. Kinetics and mechanism of the thermal decomposition reaction of 3,3-bis (azidomethyl)oxetane/tetrahydrofuran copolymer. Chin J Chem. 2004;22(11):1219–24. doi: 10.1002/cjoc.20040221102.
(16) Badgujar DM, Talawar MB, Asthana SN, Mahulikar PP. Advances in science and technology of modern energetic materials: an overview. J Hazard Mater. 2008;151(2-3):289–305. doi: 10.1016/j.jhazmat.2007.10.039.
(17) Pisharath S, Ang HG. Synthesis and thermal decomposition of GAP-Poly(BAMO) copolymer. Polym Degrad Stabil. 2007;92(7):1365–77. doi: 10.1016/j.polymdegradstab.2007.03.016.
(18) Zhang ZJ, Wang G, Wang Z, Zhang YL, Ge Z, Luo YJ. Synthesis and characterization of novel energetic thermoplastic elastomers based on glycidyl azide polymer (GAP) with bonding functions. Polym Bull. 2015;72:1835–47. doi: 10.1007/s00289-015-1375-7.
(19) Cheradame H, Andreolety JP, Rousset E. Synthesis of polymers containing pseudohalide groups by cationic polymerization, 1. Homopolymerization of 3,3-bis(azidomethyl)oxetane and its copolymerization with 3-chloromethyl-3-(2,5,8-trioxadecyl) oxetane. Makromol Chem. 1991;192(4):901–18. doi: 10.1002/macp.1991.021920414.
(20) Zhang C, Li J, Luo YJ, Zhai B. Preparation and property studies of carbon nanotubes covalent modified BAMO-AMMO energetic binders. J Energ Mater. 2015;33(4):305–14. doi: 10.1080/07370652.2014.990588.
(21) Eroglu MS, Bostan MS. GAP pre-polymer, as an energetic binder and high performance additive for propellants and explosives: a review. Org Commun. 2017;10(3):135–43. doi: 10.25135/acg.oc.21.17.07.038.
(22) Ma S, Du W, Luo Y. Simulation of GAP/HTPB phase behaviors in plasticizers and its application in composite solid propellant. E-Polymers. 2018;18(6):529–40. doi: 10.1515/epoly-2018-0012.
(23) You JS, Noh ST. Thermal and mechanical properties of poly (glycidyl azide)/polycaprolactone copolyol-based energetic thermoplastic polyurethanes. Macromol Res. 2010;18:1081–7. doi: 10.1007/s13233-010-1104-x.
(24) Ma MY, Kwon Y. Reactive energetic plasticizers utilizing Cu-free azide-alkyne 1,3-dipolar cycloaddition for *in situ* preparation of poly(THF-*co*-GAP)-based polyurethane energetic binders. Polymers. 2018;10(5):516. doi: 10.3390/polym10050516.
(25) Sun QL, Sang C, Wang Z, Luo YJ. Improvement of the creep resistance of glycidyl azide polyol energetic thermoplastic elastomer-based propellant by nitrocellulose filler and its mechanism. J Elastom Plast. 2018;50(7):579–95. doi: 10.1177/0095244317742680.
(26) Qi C, Tang G, Guo X, Liu CH, Pang AM, Gan L, et al. Network regulation and properties optimization of glycidyl azide polymer-based materials as a candidate of solid propellant binder via alternating the functionality of propargyl-terminated polyether. J Appl Polym Sci. 2019;136(40):48016. doi: 10.1002/app.48016.
(27) Miyazaki T, Kubota N. Energetics of BAMO. Propell Explos Pyrot. 1992;17(1):5–9. doi: 10.1002/prep.19920170103.
(28) Reddy TS, Nair JK, Satpute RS, Gore GM, Sikder AK. Rheological studies on energetic thermoplastic elastomers. J Appl Polym Sci. 2010;118(4):2365–8. doi: 10.1002/app.32182.
(29) Nair JK, Satpute RS, Polke BG, Mukundan T, Asthana SN, Singh H. Synthesis and characterisation of bis-azido methyl oxetane and its polymer and copolymer with tetrahydrofuran. Def Sci J. 2002;52(2):147–56. doi: 10.14429/dsj.52.2159.
(30) Hsiue GH, Liu YL, Chiu YS. Triblock copolymers based on cyclic ethers – preparation and properties of tetrahydrofuran and 3,3-bis(azidomethyl) oxetane triblock copolymers. J Polym Sci Pol Chem. 1994;32(11):2155–9. doi: 10.1002/pola.1994.080321118.
(31) Zhai JX, Yang RJ, Li JM. Catalytic thermal decomposition and combustion of composite BAMO-THF propellants. Combust Flame. 2008;154(3):473–7. doi: 10.1016/j.combustflame.2008.04.016.
(32) Jian XX, Hu YW, Zheng QL. Effect of thermal processing temperature on the microphase separation and mechanical properties of BAMO/THF polyurethane. J Polym Eng. 2017;37(2):169–76. doi: 10.1515/polyeng-2015-0509.
(33) Lv J, Huo JZ, Yang Y, Yu YF, Zhan GZ, Zhang HK. Microphase separation and thermo-mechanical properties of energetic poly(urethane-urea). Polym Bull. 2018;75:4019–36. doi: 10.1007/s00289-017-2251-4.
(34) Yilgor I, Yilgor E, Guler IG, Ward TC, Wilkes GL. FTIR investigation of the influence of diisocyanate symmetry on the morphology development in model segmented polyurethanes. Polymer. 2006;47(11):4105–14. doi: 10.1016/j.polymer.2006.02.027.
(35) Matavos-Aramyan S, Jazebizadeh MH, Babaei S. Investigating $CO_2$, $O_2$ and $N_2$ permeation properties of two new types of nanocomposite membranes: polyurethane/silica and polyesterurethane/silica. Nano-Struct Nano-Objects. 2020;21:100414. doi: 10.1016/j.nanoso.2019.100414.
(36) Saha K, Dutta K, Basu A, Adhikari A, Chattopadhyay D, Sarkar P. Controlled delivery of tetracycline hydrochloride intercalated into smectite clay using polyurethane nanofibrous membrane for wound healing application. Nano-Struct Nano-Objects. 2020;21:100418. doi: 10.1016/j.nanoso.2019.100418.